Toxicology Reports 10 (2023) 481–486

Contents lists available at ScienceDirect

Toxicology Reports

journal homepage: www.elsevier.com/locate/toxrep

Comparison of ^{1}H-magnetic resonance spectroscopy and blood biochemistry as methods for monitoring non-diffuse hepatic steatosis in a rat model

Yuka Yoshino [a,b,*], Yuta Fujii [a,b], Kazuhiro Chihara [a], Aya Nakae [b,c], Jun-ichiro Enmi [b,c], Yoshichika Yoshioka [b,c], Izuru Miyawaki [a]

[a] Preclinical Research Unit, Sumitomo Pharma Co., Ltd., 3–1-98 Kasugade-naka, Konohana-ku, Osaka 554–0022, Japan
[b] Graduate School of Frontier Biosciences, Osaka University, 1–3 Yamadaoka, Suita city, Osaka 565–0871, Japan
[c] Center for Information and Neural Networks (CiNet), Osaka University and National Institute of Information and Communications Technology (NICT), 1–4 Yamadaoka, Suita city, Osaka 565–0871, Japan

ARTICLE INFO

Handling Editor: Prof. L.H. Lash

Keywords:
Non-diffuse hepatic steatosis
Monitor
Magnetic resonance imaging
^{1}H-magnetic resonance spectroscopy
Methionine choline deficient diet
Blood biochemistry

ABSTRACT

No method of monitoring drug-induced hepatic steatosis has been established, which is a concern in drug development. Hepatic steatosis is divided into diffuse and non-diffuse forms according to the pattern of fat deposition. Diffuse hepatic steatosis was reported as evaluable by ^{1}H-magnetic resonance spectroscopy (^{1}H-MRS), which is used as an adjunct to the MRI examination. Blood biomarkers for hepatic steatosis have been also actively investigated. However, there are few reports to conduct ^{1}H-MRS or blood test in human or animal non-diffuse hepatic steatosis with reference to histopathology. Therefore, to investigate whether non-diffuse hepatic steatosis can be monitored by ^{1}H-MRS and/or blood samples, we compared histopathology to ^{1}H-MRS and blood biochemistry in a non-diffuse hepatic steatosis rat model. Non-diffuse hepatic steatosis was induced by feeding rats the methionine choline deficient diet (MCDD) for 15 days. The evaluation sites of ^{1}H-MRS and histopathological examination were three hepatic lobes in each animal. The hepatic fat fraction (HFF) and the hepatic fat area ratio (HFAR) were calculated from ^{1}H-MRS spectra and digital histopathological images, respectively. Blood biochemistry analyses included triglycerides, total cholesterol, alanine aminotransferase, and aspartate aminotransferase. A strong correlation was found between HFFs and HFARs in each hepatic lobe ($r = 0.78$, $p < 0.0001$) in rats fed the MCDD. On the other hand, no correlation was found between blood biochemistry values and HFARs. This study showed that ^{1}H-MRS parameters correlated with histopathological changes but blood biochemistry parameters didn't, so that it is suggested that ^{1}H-MRS has the potential to be a monitoring method for non-diffuse hepatic steatosis in rats fed the MCDD. Given that ^{1}H-MRS is commonly used in preclinical and clinical studies, ^{1}H-MRS should be considered a candidate method for monitoring drug-induced hepatic steatosis.

1. Introduction

Hepatic steatosis, defined as lipid accumulation in hepatocytes without other morphological findings, can be induced by drug candidates. Two types of fat deposition patterns have been reported in clinical studies: diffuse fat deposition in the entire liver and non-diffuse fat deposition in parts of the liver. The diffuse pattern is the most common, and non-diffuse patterns include geographic, focal, subcapsular, multifocal, and perivascular patterns [17,4]. When developing drug candidates that potentially induce hepatic steatosis especially with limited safety margin, there is a need for methods that can be used to monitor the occurrence and severity of hepatic steatosis in preclinical and

Abbreviations: MRI, magnetic resonance imaging; ^{1}H-MRS, ^{1}H-magnetic resonance spectroscopy; CT, computerized tomography; MCDD, methionine choline deficient diet; RARE, rapid acquisition with relaxation enhancement; TR, repetition time; TE, echo time; PRESS, point-resolved spectroscopy; HFF, hepatic fat fraction; SI, saturated fatty acid index; ALT, alanine aminotransferase; AST, aspartate aminotransferase; HE, hematoxylin and eosin; HFAR, hepatic fat area ratio; TBARS, thiobarbituric acid reactive substances; ROS, reactive oxygen species; MRI-PDFF, MRI-based proton-density-fat-fraction; SFAs, saturated fatty acids; NASH, non-alcoholic steatohepatitis.

* Correspondence to: D.V.M., Preclinical Research Unit, Sumitomo Pharma Co., Ltd., 3–1-98 Kasugade-naka, Konohana-ku, Osaka 554–0022, Japan.
E-mail address: yuka.yoshino@sumitomo-pharma.co.jp (Y. Yoshino).

https://doi.org/10.1016/j.toxrep.2023.04.007
Received 14 February 2023; Received in revised form 23 March 2023; Accepted 14 April 2023
Available online 15 April 2023

clinical studies. The gold standard for diagnosing hepatic steatosis is liver biopsy. However, it has some limitations such as hemorrhage and morbidity due to invasiveness, and sampling error due to slight heterogeneity of fat distribution in the liver [3]. Therefore, biopsy is not a suitable monitoring method and there is no established monitoring method for drug-induced hepatic steatosis.

To monitor drug-induced hepatic steatosis, blood biomarkers have been actively investigated [1], but the investigations have not focused on fat deposition pattern. On the other hand, although not safety biomarker applications, imaging modalities can depict both diffuse and non-diffuse hepatic steatosis [16]. Clinical meta-analysis suggested a preference among imaging modalities for magnetic resonance imaging (MRI) and ^{1}H-magnetic resonance spectroscopy (^{1}H-MRS) over ultrasound and computerized tomography (CT) for accurate assessment of hepatic steatosis [2]. ^{1}H-MRS is an adjunct to MRI examination, identifies signals from protons associated with triglycerides by their resonance frequencies [8], and has been widely reported to be accurately quantify hepatic steatosis [16,9]. In addition, ^{1}H-MRS allows site-specific quantification and we considered this site-specific quantification to be important and useful in non-diffuse hepatic steatosis because the evaluation in the whole liver might underestimate non-diffuse hepatic steatosis. However, there are few reports to conduct ^{1}H-MRS in human or animal non-diffuse hepatic steatosis with the reference to histopathology.

As reported in this paper, we induced non-diffuse hepatic steatosis in rats using the methionine choline deficient diet (MCDD). To our knowledge, this is the first report to establish a non-diffuse hepatic steatosis model in preclinical studies. The MCDD can be used to induce hepatic steatosis in experimental animals. Fat deposition patterns of hepatic steatosis induced by the MCDD have been rarely reported, but unlike this paper, another paper reported fat deposition throughout the hepatic lobe [12]. Rats fed the MCDD have shown decreased levels of serum cholesterol and triglycerides with diet duration, and those blood biochemistries significantly correlated with total intrahepatic triglycerides [10], suggesting that serum cholesterol and triglycerides could be used to monitor MCDD-induced hepatic steatosis. However, it was unclear whether those blood biochemistries can monitor non-diffuse hepatic steatosis induced by the MCDD.

In this study, to verify whether non-diffuse hepatic steatosis can be monitored by ^{1}H-MRS and/or blood samples, we used the MCDD-induced non-diffuse hepatic steatosis model to compare histopathological changes to changes in ^{1}H-MRS and blood biochemistry parameters.

2. Material and methods

2.1. Study design

All animal studies were approved by the Committee for the Ethical Usage of Experimental Animals of Sumitomo Pharma Co., Ltd., and the Animal Welfare Committee of Osaka University.

Fifteen female Slc:Wistar rats (five-week-old) were purchased from Japan SLC, Inc. (Shizuoka, Japan) and were allowed an acclimation period of 1 week with standard diet (CE-2, CLEA Japan, Ltd.). The rats were housed individually in a barrier-sustained room under controlled temperature of 24 ± 2 °C with relative humidity of 55 ± 10% and a 12-h light (8 a.m. to 8 p.m.)/dark cycle. The rats had free access to diet and water.

For 15 days, eleven rats in the MCDD group were fed the MCDD (Oriental Yeast Co., Ltd.) and the other four rats in the control group were fed a standard diet (CE-2, CLEA Japan, Ltd.). After fasting more than 12 h, eight rats in the MCDD group and all rats in the control group were subjected to a series of examinations including ^{1}H-MRS, histopathology, and blood biochemistry. In the remaining three animals in the MCDD group, histopathological examination and blood biochemistry were conducted after fasting.

2.2. In vivo MRI and ^{1}H-MRS

All MRI and ^{1}H-MRS examinations were performed using an 11.7 T vertical-bore Bruker Avance II imaging system (Bruker BioSpin, Ettlingen, Germany) and a 33 mm volume radiofrequency coil for transmission and reception (Bruker BioSpin, Ettlingen, Germany). The rats were anesthetized with 1–2% isoflurane (Wako, Osaka, Japan). The respiration rate was monitored using a physiological monitoring system (SA Instruments, Stony Brook, NY, USA), and body temperature was kept at 36.0 ± 0.5 °C by circulating water through heating pads throughout the MRI and ^{1}H-MRS examinations. To position the spectroscopic voxel for ^{1}H-MRS, coronal, axial, and sagittal T2-weighted images through the liver were acquired using a rapid acquisition with relaxation enhancement (RARE) sequence with the following scanning parameters: Rare Factor 16, repetition time/echo time (TR/TE) 5000 msec/51 msec, field of view 30 × 30 mm, matrix of 256 × 256 pixels, 20 slices with thickness = 1.0 mm, and 4 NEX. The voxels were confirmed to be located within the liver by coronal, axial, and sagittal T2-weighted images and placed avoiding major hepatic blood vessels in the left lateral, right lateral, and caudate hepatic lobes. Single-voxel MR spectroscopic data were acquired with a point-resolved spectroscopy (PRESS) sequence with the following parameters: TR/TE 5000 msec/11 msec, voxel dimensions 2 × 2 × 2 mm^{3}, spectral width = 4000 Hz, 8 K data points, 8 NEX, and no water suppression.

The ^{1}H-MRS data were analyzed using the LCModel software (version 6.3–1 L; Stephen Provencher, Oakville, Ontario, Canada) with SPTYPE 'liver-11′ [14] to automatically quantify the area under the peak. The resonance area we used in calculation was only those with the estimated standard deviation of less than 5%. The hepatic fat fraction (HFF) in ^{1}H-MRS was calculated as the area under the methylene -$(CH_2)_n$- peak at 1.3 ppm divided by the sum of the area under the methylene -$(CH_2)_n$- peak at 1.3 ppm and the area under the water peak at 4.7 ppm. In addition, saturated fatty acid index (SI) was calculated according to the previous report [7].

2.3. Blood biochemistry

After ^{1}H-MRS or fasting, the rats were euthanized by exsanguination under anesthesia using isoflurane. Blood samples from the MCDD group were placed in Capiject II blood collection tubes (with heparin lithium; Terumo Co., Ltd., Tokyo, Japan) and then centrifuged to obtain plasma. Triglycerides, total cholesterol, alanine aminotransferase (ALT), and aspartate aminotransferase (AST) in plasma were determined by using an automated analyzer JCA-ZS050 (JEOL Ltd., Tokyo, Japan).

2.4. Histopathological examination

After the blood sampling, the livers were dissected, and fixed in 10% neutral-buffered formalin. The left lateral, right lateral, and caudate hepatic lobes were embedded in paraffin, sectioned, and stained with hematoxylin and eosin (HE), and examined by light microscopy. Each liver was dissected in the approximate plane of maximum cross-sectional area. In addition, to calculate the hepatic fat area ratio (HFAR) in each hepatic lobe in the MCDD group, the entire histopathology slides were scanned using an Aperio AT2 whole digital slide scanner. We adjusted the parameters of the Aperio Imagescope nuclear algorithm (Leica Biosystems Imaging Inc., Vista, CA, USA) to detect the vacuoles and to quantify the fat area. In addition, we adjusted the parameters of the positive pixel count algorithm from Aperio Imagescope to detect the HE stained positive tissue area and to quantify the area without vacuoles. The HFAR was calculated as the vacuole area divided by the sum of the vacuole area and the area of HE-stained positive tissue in each hepatic lobe.

2.5. Statistics

Correlations between HFAR and HFF, HFAR and triglycerides, HFAR and total cholesterol, HFAR and ALT, HFAR and AST, and HFF and SI were evaluated with the Spearman coefficient (r). P value < 0.05 was considered to indicate a significant difference. All statistical analyses were performed by using GraphPad Prism 9.3.1 (GraphPad Software Inc., San Diego, CA, USA).

3. Results

3.1. Gross pathological and histopathological examination

Grossly, the livers were partially pale in 8/11 animals in the MCDD group and not abnormal in the rest of the animals. A typical image showed pale left lateral, left medial, and caudate hepatic lobes and no abnormalities in other lobes (Fig. 1A and B).

Histologically, the left lateral and caudate hepatic lobes showed mild to severe steatosis and the right lateral hepatic lobe showed no or minimal to mild steatosis in the MCDD group. In some animals, histopathology showed obvious heterogeneity in hepatic fat deposition in one hepatic lobe (Fig. 1C). Fat deposition was characterized by macrovesicular droplets predominantly in the centrilobular zone (Fig. 1D, E, and F). No steatosis was observed in the liver in the control group.

The HFARs were higher in the left lateral and caudate hepatic lobes than in the right lateral lobes in all animals in the MCDD group. The mean HFARs in the left lateral, caudate, and right lateral hepatic lobes were 0.14 ± 0.11, 0.09 ± 0.09 and 0.01 ± 0.01, respectively (Fig. 2). Correlations of HFARs with HFFs, and the values of triglycerides, total cholesterol, ALT, or AST described below were calculated using these individual HFARs.

Typical gross image of the anterior aspect (A) and visceral surface (B) of liver in the MCDD group. The left lateral (white arrow), left medial (black arrow), and caudate (green arrow) hepatic lobes were pale and the other lobes had no abnormality. Bar, 1 cm. Representative HE stained sections at lower magnification (C) and higher magnification (D-F) in one representative animal in the MCDD group. At lower magnification, the upper left, lower left, and right hepatic lobes correspond to the left lateral, right lateral, and caudate hepatic lobes, respectively. More vacuoles were observed in the area indicated by white arrowheads than in the area indicated by black arrowheads in the same hepatic lobe, demonstrating the heterogeneity of fat deposition in one hepatic lobe. Bar, 4 mm. At higher magnification, severe, mild, and no macrovesicular steatosis predominantly in the centrilobular zone were observed in the left lateral (D), caudate (E), and right lateral (F) hepatic lobes, respectively. Bar, 200 μm.

Dots of one color indicate data from the same animal and the bars indicate the mean values.

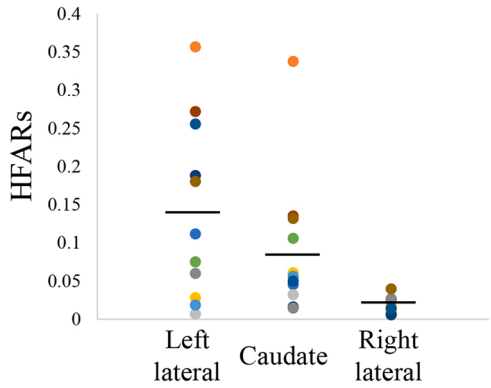

Fig. 2. Hepatic fat area ratios (HFARs) calculated from histopathological images of the left lateral, caudate, and right lateral hepatic lobes in the methionine choline deficient diet (MCDD) group.

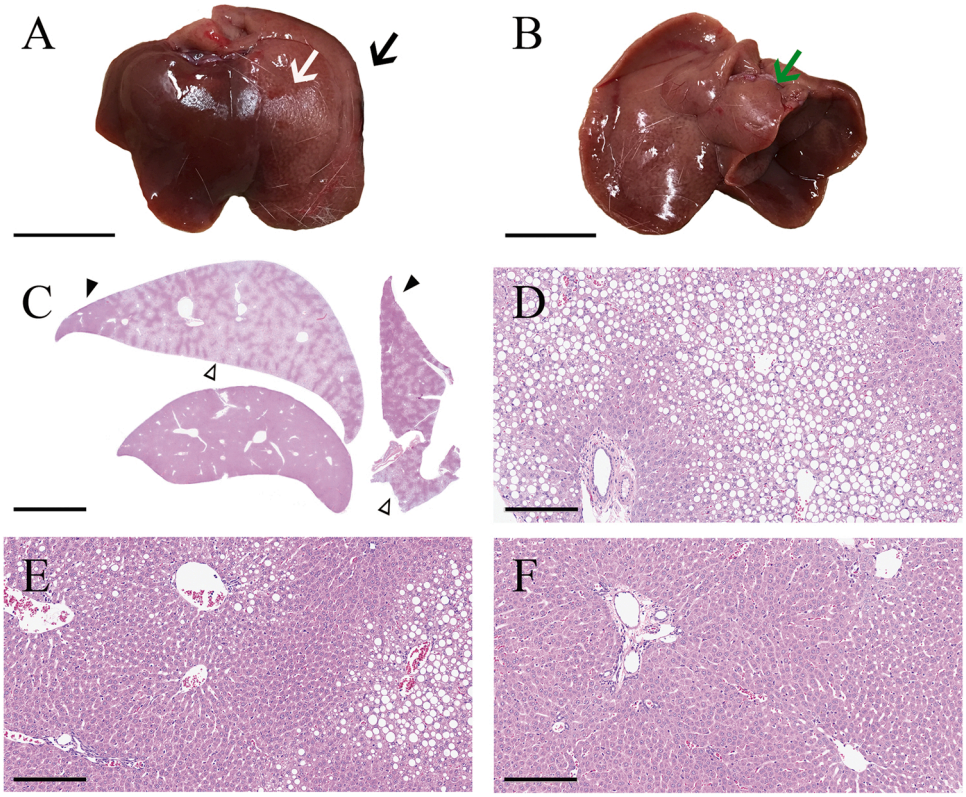

Fig. 1. Gross and histopathological images in the methionine choline deficient diet (MCDD) group.

3.2. In vivo MRI and ^{1}H-MRS

In the liver of all animals in the MCDD group, non-diffuse high intensity signals in T2-weighted images were observed. This signal intensity was higher in the left lateral and caudate hepatic lobes and lower or not observed in the right lateral hepatic lobe (Fig. 3A, B, and C). No abnormal finding was observed in T2-weighted images in the control group.

In the MCDD group, up to nine distinct fat peaks at from 0.9 to 5.3 ppm and the water peak at 4.7 ppm were resolved in the hepatic lobe with hyperintense signal in T2-weighted images (Fig. 4). In the control group, only the water peak at 4.7 ppm was detected (data not shown) with the estimated standard deviation of less than 5%, suggesting that little fat was deposited in the liver.

The mean HFFs calculated from ^{1}H-MRS in the left lateral, caudate, and right lateral lobes in the MCDD group were 0.40 ± 0.17, 0.26 ± 0.19, and 0.01 ± 0.03, respectively. A strong correlation was found between HFFs and HFARs in each hepatic lobe ($r = 0.78$, $p < 0.0001$) (Fig. 5). The mean SIs in the left lateral and caudate hepatic lobes in the MCDD group were 0.72 ± 0.11, and 0.73 ± 0.11, respectively. The SIs in the right lateral hepatic lobes in the MCDD groups were not calculated because the resonance area needed for calculation was not observed with the estimated standard deviation of less than 5%. No correlation was found between HFF and SI ($r = 0.20$, $p = 0.61$).

Typical axial T2-weighted images in the liver in the MCDD group show hyperintensity in the left lateral and caudate hepatic lobes, but not in the right lateral hepatic lobe. Square shows the MRS voxel positions in the left lateral (A), caudate (B), and right lateral (C) hepatic lobes.

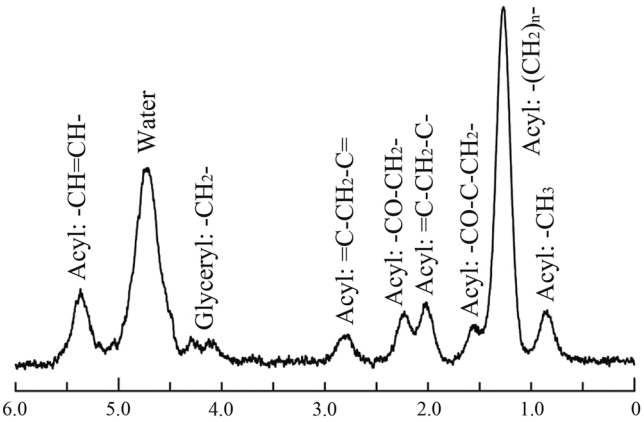

Fig. 4. Representative example of ^{1}H-MRS spectra in the methionine choline deficient diet (MCDD) group.

Lipid resonances were associated with following functional groups: Acyl: -CH_3 at 0.9 ppm, Acyl: -$(CH_2)_n$- at 1.3 ppm, Acyl: -CO-C-CH_2- at 1.6 ppm, Acyl: =C-CH_2-C- at 2.1 ppm, Acyl: -CO-CH_2- at 2.3 ppm, Acyl: =C-CH_2-C= at 2.8 ppm, Glyceryl: -CH_2- at 4.1 ppm and 4.3 ppm, and Acyl: -CH=CH- at 5.3 ppm. Water peak was observed at 4.7 ppm. Hepatic fat fraction (HFF) was calculated as the area under the peak at 1.3 ppm divided by the sum of the area under the peak at 1.3 ppm and the area under the water peak at 4.7 ppm.

A strong correlation was found between HFFs and HFARs (Spearman coefficient, $r = 0.78$, $p < 0.0001$).

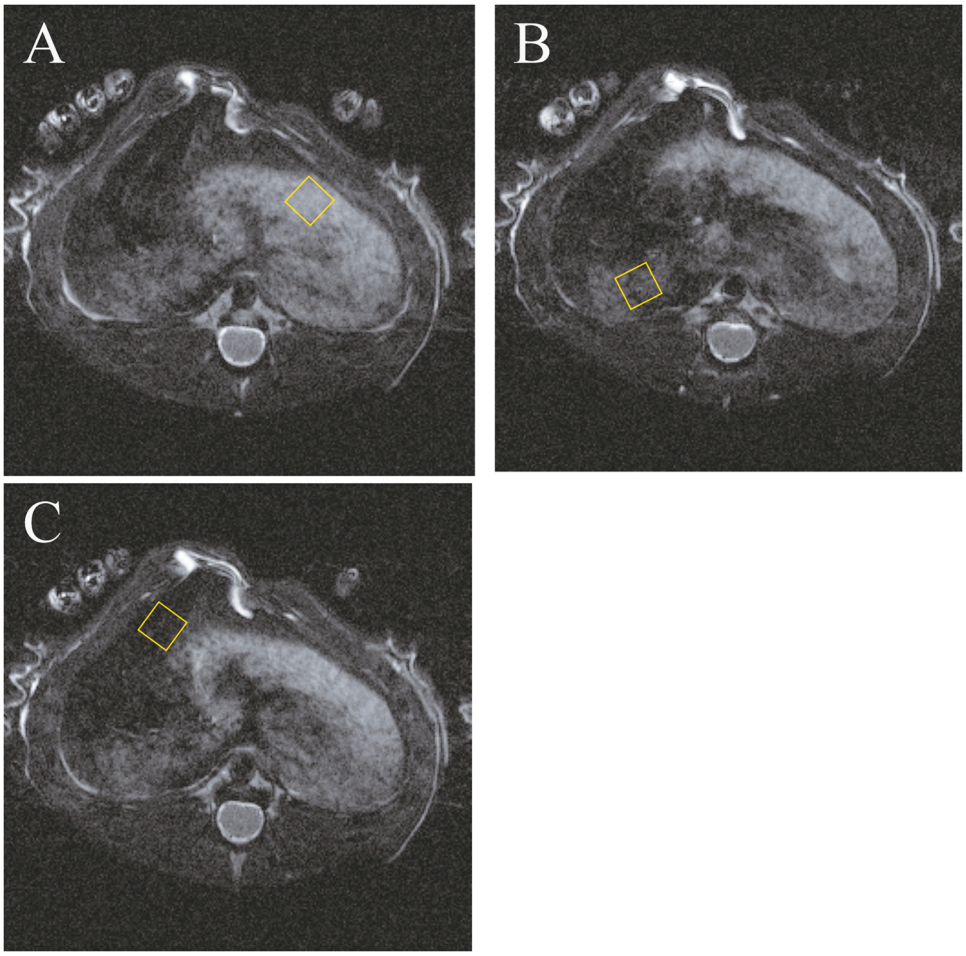

Fig. 3. Axial T2-weighted images and ^{1}H-MRS voxel positions in the liver in one representative animal in the methionine choline deficient diet (MCDD) group.

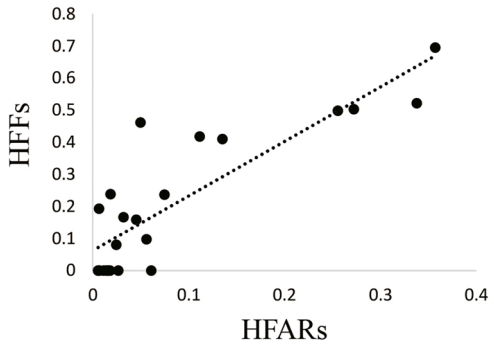

Fig. 5. Graph showing a correlation between hepatic fat fractions (HFFs) calculated from ^{1}H-MRS and hepatic fat area ratios (HFARs) calculated from histopathological images of each hepatic lobe in the methionine choline deficient diet (MCDD) group.

3.3. Blood biochemistry

In the MCDD group, the mean values of triglycerides, total cholesterol, ALT, and AST were 19.55 ± 5.88 mg/dL, 65.73 ± 9.05 mg/dL, 75.09 ± 49.94 U/L, and 144.73 ± 72.33 U/L, respectively. No correlation was found between the values of triglycerides, total cholesterol, ALT, or AST and individual mean HFAR. No correlation was also found between the values of triglycerides, total cholesterol, ALT, or AST and HFAR in the highest fat deposits in each animal (Table 1).

4. Discussion

To our knowledge, this is the first report to assess non-diffuse hepatic steatosis by using an imaging modality, histopathological examination, and blood samples. Furthermore, this is also the first report to show that HFFs, but not blood biochemistry values, significantly correlated with HFARs in rats with non-diffuse hepatic steatosis.

In the present study, non-diffuse hepatic steatosis was observed in the MCDD group. The cause of non-diffuse hepatic steatosis in the MCDD group is unknown, but functional heterogeneity among hepatic lobes may be involved [13]. For example, after Wistar rats were fed the MCDD for 8 weeks, the levels of thiobarbituric acid reactive substances (TBARS), a marker of lipid peroxidation, were significantly higher in the left hepatic lobes than in the median and right hepatic lobes. In addition, in Wistar rats fed a standard diet, reactive oxygen species (ROS) content and the level of TBARS were significantly higher in the left hepatic lobes than in the right hepatic lobes [13]. Given that excessive ROS could induce hepatic steatosis [18], high ROS in the left hepatic lobes may have been involved in high fat deposition in the left lateral hepatic lobe in the present study.

HFFs were significantly correlated with HFARs in the present study, suggesting that ^{1}H-MRS is useful for monitoring non-diffuse hepatic steatosis. Marsman et al. have already shown that ^{1}H-MRS was significantly correlated with histopathological evaluation in a rat hepatic steatosis model induced by the MCDD [11]. However, Marsman et al. studied diffuse hepatic steatosis on MRI, not non-diffuse hepatic steatosis, thus this is the first report to show that evaluation by ^{1}H-MRS in multiple hepatic lobes significantly correlated with histopathological evaluation in the corresponding hepatic lobes in non-diffuse hepatic steatosis. In addition, this study and Marsman et al.'s study showed that ^{1}H-MRS can accurately quantify hepatic steatosis regardless of the fat deposition pattern. Drug-induced hepatic steatosis can be either diffuse or non-diffuse. Therefore, ^{1}H-MRS is considered to be a useful method for monitoring drug-induced hepatic steatosis.

Table 1
Correlation between blood biochemistry and HFAR in the MCDD group.

	vs mean HFAR		vs highest HFAR	
	r	p	r	p
Triglycerides	0.12	0.73	0.14	0.69
Total cholesterol	0.29	0.38	0.34	0.30
ALT	0.39	0.24	0.36	0.27
AST	0.06	0.86	0.08	0.82

MCDD: methionine choline deficient diet, HFAR: hepatic fat area ratio, r: Spearman coefficient, ALT: alanine aminotransferase, AST: asparate aminotransferase

Non-diffuse hepatic steatosis could be evaluated using ^{1}H-MRS because the ROIs were drawn small enough to fit in one hepatic lobe by using high-field MRI. Small ROIs made it possible to conduct ^{1}H-MRS at multiple sites without duplication. Since the ROI is generally in one hepatic lobe in clinical settings, it is important to use high-field MRI in nonclinical settings and a ^{1}H-MRS technique similar to that used clinically. In addition, the operator can choose where to place the ROIs in the liver in ^{1}H-MRS. This is considered to be advantage especially when evaluating non-diffuse hepatic steatosis. By placing the voxel in the higher intensity sites in T2-weighted image, we may be able to quantify the highest fat deposition in the individual. Increase in some lipids including saturated fatty acids (SFAs) may lead the induction of non-alcoholic steatohepatitis (NASH) as discussed below [5,6]. Therefore, the ability to assess the highest fat deposition in the individual, that ^{1}H-MRS may have, was considered to be important for monitoring non-diffuse hepatic steatosis.

In the graphs showing the correlation between HFF and HFAR, some plots deviated from a linear relationship. A possible reason for this deviation was that the sites used for histopathological and ^{1}H-MRS evaluation did not perfectly match, even within the same hepatic lobe. In this rat model, heterogeneity in hepatic fat deposition was obvious not only between hepatic lobes, but also within one hepatic lobe. Therefore, evaluation site inconsistencies may have affected the evaluation of non-diffuse hepatic steatosis more than the evaluation of non-diffuse hepatic steatosis. In addition, limitations exist that are due to differences in the principles used to measure HFFs and HFARs: the lipid index used in HFF was the ratio of mobile water to mobile triglycerides in a specified tissue volume, whereas the lipid index used in HFAR was the ratio of liver tissue to vacuoles in a specified tissue area.

The values of blood biochemistries were not correlated with HFARs under the conditions of the present study. However, Leiber et al. reported that the values of blood triglycerides and total cholesterol were significantly and negatively correlated with those of total intrahepatic triglycerides, which were measured by biochemical analysis using a part of the homogenized liver tissue. In addition, total intrahepatic triglycerides were significantly correlated with HFFs calculated from histopathological images [10]. The difference between Leiber et al. and us in the correlation between blood biochemistry and HFAR might be related to the pattern of fat deposition.

Although fat deposition patterns have not been clearly differentiated, the MRI results reported by Leiber et al. indicate that diffuse hepatic steatosis has been observed. Also small differences in fat content between hepatic lobes have been reported in patients with diffuse hepatic steatosis [3], but it is obvious that these differences are smaller than those observed in non-diffuse hepatic steatosis. Therefore, given that the values of blood parameters reflect the overall condition of the liver, it is considered that no correlation between blood biochemistry and HFAR in the present study might be due to the non-diffuse pattern of fat deposition. Further studies with additional number of animals are warranted to confirm the reproducibility.

As well as ^{1}H-MRS used in the present study, MRI-based proton density fat fraction (MRI-PDFF) can also be used to quantify the HFFs through analysis of chemical shifts between water and fat proton signals. HFFs in MRI-PDFF analysis were calculated from the fat and water component images. Not only HFFs in ^{1}H-MRS but also in MRI-PDFF analysis showed a strong correlation with the histopathologic parameters in the evaluation of hepatic steatosis [9]. An advantage of ^{1}H-MRS

over MRI-PDFF is the ability to depict distinct fat peaks. Up to nine and six distinct fat peaks can be observed in high-resolution spectroscopy and in clinical field-resolution spectroscopy, respectively. Since the fat peaks blend together in clinical field-resolution, the number of fat peaks is reduced compared to that in high-resolution spectroscopy [15]. By using these peaks, saturated, unsaturated, and polyunsaturated fatty acid indices could be measured [7]. In the present study, SI was calculated and didn't correlate with HFF, suggesting that SI might not necessarily increase proportionally as total fat deposition increases. Not all but some lipids including SFAs are considered to be toxic and could be involved in the progression of hepatic steatosis to NASH [6]. Hepatic SFAs were increased in NASH patients compared with control and hepatic steatosis patients, and high concentration of SFAs were hepatotoxic in vitro [5]. These findings suggest that increases in SFAs in specific parts of the liver may lead to induction of NASH at the same site. Therefore, the ability to depict distinct fat peaks, which is an advantage of ^{1}H-MRS over MRI-PDFF, may be used not only for monitoring hepatic steatosis but also as a biomarker of NASH. Further studies are required to show that ^{1}H-MRS can detect the progression of hepatic steatosis to NASH.

In conclusion, this study showed that ^{1}H-MRS parameters, but not blood biochemistry parameters, correlated with the histopathological changes in rats fed the MCDD. ^{1}H-MRS is considered to have the potential to accurately quantify both diffuse and non-diffuse hepatic steatosis, which can be observed in drug-induced hepatic steatosis, and can be commonly used in preclinical and clinical studies. Therefore, ^{1}H-MRS is considered to be a candidate method for monitoring drug-induced hepatic steatosis.

Funding

This work was supported by Sumitomo Pharma Co., Ltd.

CRediT authorship contribution statement

Yuka Yoshino: Conceptualization, Methodology, Formal analysis, Investigation, Visualization, Writing – original draft **Yuta Fujii:** Conceptualization, Methodology, Investigation, Writing – review & editing **Kazuhiro Chihara:** Conceptualization, Supervision, Writing – review & editing **Aya Nakae:** Conceptualization, Supervision, Writing – review & editing **Jun-ichiro Enmi**: Conceptualization, Methodology, Formal analysis, Investigation, Supervision, Writing – review & editing **Yoshichika Yoshioka:** Conceptualization, Methodology, Formal analysis, Investigation, Supervision, Visualization, Writing – review & editing **Izuru Miyawaki:** Conceptualization, Supervision, Writing – review & editing.

Declaration of Competing Interest

The authors declare that they have no known competing financial interests or personal relationships that could have appeared to influence the work reported in this paper.

Data availability

Data will be made available on request.

References

[1] D.E. Amacher, Strategies for the early detection of drug-induced hepatic steatosis in preclinical drug safety evaluation studies, Toxicology 279 (1–3) (2011) 10–18.
[2] A.E. Bohte, J.R. van Werven, S. Bipat, J. Stoker, The diagnostic accuracy of US, CT, MRI and ^{1}H-MRS for the evaluation of hepatic steatosis compared with liver biopsy: a meta-analysis, Eur. Radio. 21 (1) (2011) 87–97.
[3] S. Bonekamp, A. Tang, A. Mashhood, T. Qolfson, C. Changchien, M.S. Middleton, L. Clark, A. Gamst, R. Loomba, C.B. Sirlin, Spatial distribution of MRI-determined hepatic proton density fat fraction in adults with nonalcoholic fatty liver disease, J. Magn. Reson Imaging 39 (6) (2014) 1525–1532.
[4] L. Calistri, V. Rastrelli, C. Nardi, D. Maraghelli, S. Vidali, M. Pietragalla, S. Colagrande, Imaging of the chemotherapy-induced hepatic damage: yellow liver, blue liver, and pseudocirrhosis, World J. Gastroenterol. 27 (46) (2021) 7866–7893.
[5] F. Chiappini, A. Coilly, H. Kadar, P. Gual, A. Tran, C. Desterke, D. Samuel, L. C. Duclos-Vallée, D. Touboul, J. Bertrand-Michel, A. Brunelle, C. Guettier, F. L. Naour, Metabolism dysregulation induced a specific lipid signature pf nonalcoholic steatohepatitis in patients, Sci. Rep. 24 (7) (2017) 46658.
[6] Y. Geng, K.N. Faber, V.E. de Meijer, H. Blokzijl, H. Moshage, How dose hepatic lipid accumulation lead to lipotoxicity in non-alcoholic fatty liver disease? Hepatol. Int 15 (1) (2021) 21–35.
[7] N.A. Johnson, D.W. Walton, T. Sachinwalla, C.H. Thompson, L. Smith, P.A. Ruell, S.R. Stannard, J. George, Noninvasive assessment of hepatic lipid composition: advancing understanding and management of fatty liver disorders, Hepatology 47 (5) (2008) 1513–1523.
[8] S. Kechagias, M. Ekstedt, C. Simonsson, P. Nasr, Non-invasive diagnosis and staging of non-alcoholic fatty liver disease, Horm. (Athens) 21 (3) (2022) 349–368.
[9] J.W. Kim, C.H. Lee, Z. Yang, B.H. Kim, Y.S. Lee, K.A. Kim, The spectrum of magnetic resonance imaging proton density fat fraction (MRI-PDFF), magnetic resonance spectroscopy (MRS), and two different histopathologic methods (artificial intelligence vs. pathologist) in quantifying hepatic steatosis, Quant. Imaging Med Surg. 12 (11) (2022) 5251–5262.
[10] L.M. Leiber, J. Bourisier, S. Michalak, V. Roullier, L. Fizanne, J. Chaigneau, J. Roux, V. Moal, M. Flamment, P. Bazeries, P.-H. Ducluzeau, C. Aube, MRI versus histological methods for time course monitoring of steatosis amount in a murine model of NAFLD, Diagn. Inter. Imaging 96 (9) (2015) 915–922.
[11] H.A. Marsman, J.R. van Werven, A.J. Nederveen, F.J. Ten Kate, M. Heger, J. Stoker, T.N. van Gulik, Noninvasive quantification of hepatic steatosis in rats using 3.0T ^{1}H-magnetic resonance spectroscopy, J. Magn. Reson Imaging 32 (1) (2010) 148–154.
[12] Y. Miyata, T. Miyahara, F. Moriyasu, Decreased accumulation of ultrasound contrast in the liver of nonalcoholic steatohepatitis rat model, World J. Gastroenterol. 17 (37) (2011) 4191–4198.
[13] G. Palladini, L.G. Pasqua, C. Berardo, V. Siciliano, P. Richelmi, S. Perlini, A. Ferrigno, M. Vairetti, Animal models of steatosis (NAFLD) and steatohepatitis (NASH) exhibit hepatic lobe-specific gelatinases activity and oxidative stress, Can. J. Gastroenterol. Hepatol. (2019) 5413461.
[14] S.W. Provencher, Estimation of metabolic concentrations from localized in vivo proton NMR spectra, Magn. Reson. Med. 30 (1993) 672–679.
[15] S.B. Reeder, I. Cruite, G. Hamilton, C.B. Sirlin, Quantitative assessment of liver fat with magnetic resonance imaging and spectroscopy, J. Magn. Reson Imaging 34 (4) (2011) 729–749.
[16] L.S. Szczepaniak, P. Nurenberg, D. Leonard, J.D. Browning, J.S. Reingold, S. Grundy, H.H. Hobbs, R.L. Dobbins, Magnetic resonance spectroscopy to measure hepatic triglyceride content: prevalence of hepatic steatosis in the general population, Am. J. Physiol. Endocrinol. Metab. 288 (2) (2005) E462–E468.
[17] S.K. Venkatesh, T. Hennedige, G.B. Johnson, D.M. Hough, J.G. Fletcher, Imaging patterns and focal lesions in fatty liver: a pictorial review, Abdom. Radio. (NY) 42 (5) (2017) 1374–1392.
[18] L. Zhang, X. Wang, R. Cueto, C. Effi, Y. Zhang, H. Tan, X. Qin, Y. Ji, H. Wang, Biochemical basis and metabolic interplay of redox regulation, Redox Biol. 26 (2019), 101284.